ijlpr 2022; doi 10.22376/ijpbs/lpr.2022.12.3.L40-50

International Journal of Life science and Pharma Research
ISSN 2250-0480

Research Article

Chemistry For New Drug Discovery

Inhibitive Effect of Organic Inhibitors on the Corrosion of Mild Steel in Acidic Medium

P.Singaravelu[1]*, N. Bhadusha[1] and V.Dharmalingam[2]

*[1]*Research Scholar, Department of Chemistry, Government Arts College (Autonomous), Salem - 636007, Tamilnadu, India.*
[1]Assistant Professor, Department of Chemistry, Government Arts College (Autonomous), Salem - 636007, Tamilnadu, India.
[2]Assistant Professor, Department of Chemistry, Mahendra Engineering College (Autonomous), Namakkal - 637503, Tamilnadu, India.

Abstract: The aim of the present work was to study the corrosion inhibition of mild steel using organic inhibitors. The corrosion inhibition activity of a newly synthesized [4-(4-aminobenzoyl) piperazin-1-yl) (furan-2-yl) methanone (4-4-ABPFM) and [4-(4-aminophenyl) piperazin-1-yl) (furan-2-yl) methanone (4-4-APFM) was investigated on the corrosion of mild steel in 1N HCl at room temperature for two hours using different methods.Such as weight loss, potentiodynamic polarization and electrochemical impedance spectroscopy (EIS). Organic Inhibitor (4-4-ABPFM) were prepared throughout condensation of hydrochloric acid and reduction reaction using the reagent $SnCl_2$, compound (4-4-APFM) involved a two reaction sequence of nucleophilic aromatic substitution and nitro group reduction, characterized by Fourier transform infrared spectroscopy (FT-IR). Electrochemical polarization test was also conducted to confirm the effectiveness of inhibition. Morphology of sample surfaces was respectively examined by scanning electron microscope (SEM). The result shows that the inhibition efficiency increases significantly up to 80% [4-(4-aminobenzoyl) piperazin-1-yl) (furan-2-yl) methanone (4-4-ABPFM) and 73% [4-(4-aminophenyl) piperazin-1-yl) (furan-2-yl) methanone (4-4-APFM). The optimum efficiency is obtained at (4-4-ABPFM) concentration of 100 ppm for expositing time of 2 hours at room temperature. The polarization curve shows the inhibitor behaves as a mixed inhibitor with the dominant cathodic inhibition. The adsorption of optimum concentration of both the inhibitor on the surface of mild steel in 1N HCl solution follows Langmuir adsorption isotherm. The Surface condition is improved due to the adsorption and then formation of thin layer film protection in the surface of the mild steel. The synthesized compounds show an appreciable corrosion inhibition property for mild steel in 1N HCl medium at room temperature which varies in the order: (4-4-APFM) < (4-4-ABPFM) compound.

Keywords: Organic inhibitors, Mild steel, Electrochemical studies, Adsorption, FT-IR, SEM

***Corresponding Author**

P.Singaravelu , Research Scholar, Department of Chemistry,
Government Arts College (Autonomous), Salem - 636007,
Tamilnadu, India.

Received On **27 December, 2021**
Revised On **17 March, 2022**
Accepted On **25 March, 2022**
Published On 2 May, 2022

Funding This research did not receive any specific grant from any funding agencies in the public, commercial or not for profit sectors.

Citation P.Singaravelu, N. Bhadusha and V.Dharmalingam , Inhibitive Effect of Organic Inhibitors on the Corrosion of Mild Steel in Acidic Medium.(2022).Int. J. Life Sci. Pharma Res.12(3), L40-50 http://dx.doi.org/10.22376/ijpbs/lpr.2022.12.3.L40-50

1. INTRODUCTION

Mild steel is used in many industrial and structural applications due to its good mechanical strength and relatively low cost[1,2]. Acidic solutions commonly used in many industrial activities, including the steelmaking finishing process, constitute unfriendly corrosive media for mild steel[3]. The use of organic corrosion inhibitors has been identified as one of the most economical ways of reducing corrosion rate and protecting steel-made industrial facilities against corrosion. Mild steel undergoes severe corrosion in pickling processes. Hydrochloric and sulfuric acids are widely used for pickling and descaling of mild steel[4]. Generally, the heterogeneous organic compounds having higher basicity and electron density on the hetero atoms such as N, O, and S, have tendency to resist corrosion. Nitrogen and oxygen are the active centers for the process of adsorption on the metal surface. These compounds can adsorb on the metal surface, block the active sites on the surface and thereby reduce the corrosion attack. The efficiency of these compounds as corrosion inhibitors can be attributed to the number of mobile electron pairs present, the p orbital character of free electrons and the electron density around nitrogen and oxygen atoms[5-7]. In a recent year, many researchers synthesized many organic compounds and they were utilized as corrosion inhibitors in various acidic mediums. A research article stated that 5-Amino-2-chloro-3-Picoloine (ACP) corrosion inhibitor was used in 1.11N HCl medium which shows inhibition efficiency of 85.39%[8]. Using Formazan derivative products were synthesized and used as an inhibitor in 1.11N HCl medium at three different temperatures it shows IE at 303K -79.21%, 353K-67.94% and 403K-60.67%[9]. In 1M sulphuric acid and 1M HCl, a group of oxadiazoles compounds were used as corrosion inhibitors where the efficiency denoted >90 % in 1M HCl than in 1 M sulfuric acid (IE%-70)[10]. Inhibition efficiency 96.8% of Schiff's base triazole compound against 1M HCl was identified and reported[11]. Previously existing data show that organic compounds act by forming surface film at metal/electrolyte interfaces[12, 13]. Generally, adsorption of these inhibitors is influenced by numerous factors including chemical structure, electronic distribution, and nature of metal and testing medium[14]. Literature survey reveals that heterocyclic's containing nitrile groups act as efficient corrosion inhibitors for metals in different testing media[15–17]. The selection of inhibitors for different processes is screened for various reasons by considering its availability and nontoxicity. This is in combination with the specific characteristics of many corrosion retarding substances, which partially demands the mixed mode inhibitors obtain high corrosion inhibition. Considering costs of most common corrosion inhibitors, recently researchers focused on identifying new groups of inexpensive and effective inhibitors to address future environmental and safety needs. Hence, the identification of drugs as effective corrosion inhibitors for metals in acidic medium has paid good attention[18–21]. Therefore, keeping an eye on the industrial and environmental scenarios, the present study deals with the synthesis of two organic inhibitors namely [4-(4-aminobenzoyl) piperazin-1-yl)(furan-2-yl)methanone (4-4-ABPFM) and [4-(4-aminophenyl)piperazin-1-yl)(furan-2-yl) methanone (4-4-APFM) and their application for the first time as corrosion inhibitors on mild steel in 1N HCl medium time of 2 hours at room temperature in the concentration range of 10 ppm to 100 ppm. The inhibitive activity of (4-4-ABPFM) and (4-4-APFM) is examined successively via weight loss measurement, Fourier transform infrared spectroscopy (FT-IR), electrochemical impedance spectroscopy (EIS), potentiodynamic polarization, Langmuir isotherm calculation, scanning electron microscopy (SEM).

2. MATERIALS AND METHODS

2.1 *Materials used for Corrosion Studies*

Most commonly used mild steel specimens with the following composition were Fe = 99.720, Ni = 0.017, Mo = 0.016, Cr = 0.049, S = 0.014, p = 0.017, Si = 0.009, Mn = 0.142, C = 0.016. According to ASTM[22] the specimens were cut into 5cm x 1cm size and punched a hole at the top with numbers for immersing into the test sample. In order to remove the dust the specimens were subject into a pickling bath of specific composition, which contains Con.HCl – 1 lit, Sb_2O_3 – 20g, $SnCl_2.2H_2O$ – 50 g at a room temperature (30° C) for about 20-30 mines.

2.1.1 *Testing Sample*

Triethylamine, stannous chloride, 4-fluoronitrobenzene, 1-(2-furoyl) piperazine, potassium carbonate and other reagents used analytical grade chemicals. All the solutions were prepared by using AR grade and by using doubled distilled water. 1N HCl solution was prepared by diluting 89mL of 11.3N HCl to 1000mL. Inhibitor Solutions: Using the crude synthesized organic compound [4-(4aminobenzoyl)piperazin-1-yl)(furan-2-yl)methanone (4-4-ABPFM) and [4-(4-aminophenyl)piperazin-1-yl)(furan-2-yl)methanone (4-4-APFM) were prepared by dissolving 1gm respectively in one liter of 1 N HCl. This stock solution was diluted to 10, 20, 40, 60, 80, and 100 ppm using 1 N HCl solution.

2.1.2 *Weight Loss Method*

As per the procedure, MS specimens were cut according to the ASTM standard. The material was pickled in a pickling solution and dried in desiccators. Specimens were stored in desiccators after taking the initial weight and each run of the weight loss method was carried out in 100 mL of a beaker containing test solution with and without inhibitor. A similar procedure was carried out for both inhibitors for two hours at room temperature. Using the following equations readings were calculated.

$$\text{Corrosion rate } K = \frac{8.76 \times 10000\ W}{ATD}$$

$$\text{Inhibition efficiency } IE\% = \frac{W_U - W_I}{W_U} \times 100$$

Where, T is a time of exposure in h, W is a weight loss[26] of test specimen in g, A is an area of the test specimen in cm^2, D is the density of material in g cm^3.

2.2 Adsorption parameters

Adsorption parameters such as the adsorption of free energy (ΔG_{ads}), adsorption of enthalpy (ΔH_{ads}) and entropy of adsorption (ΔS_{ads}) were calculated using Langmuir adsorption isotherm, which is presented by the following[4].

$$\boxed{\frac{C_{inh}}{\theta} = \frac{1}{K_{ads}} + C_{inh}}$$

Where C_{inh} is the inhibitor concentration, K_{ads} is the equilibrium constant, θ is surface coverage.

$$\boxed{\log\left(\frac{\theta}{1-\theta}\right) = \log A + \log C_{inh} - \frac{Q_{ads}}{2.303RT}}$$

Where, A is a constant, Q_{ads} is the heat of adsorption or enthalpy of adsorption.

Equilibrium constant $K_{ads}$was calculated from the intercepts ($1/K_{ads}$) of the straight line obtained from the plot of C_{inh}/θ Vs C_{inh}. The free energy of adsorption was calculated by substituting the equilibrium constant value in the equation.

$$\boxed{\Delta G_{ads} = -RT\ln(55.5K_{ads})}$$

The plot of log (θ /1-θ) Vs 1000 / T at various concentrations of inhibitors yield a straight line. The slope of the straight line is $-\Delta H_{ads}/2.303R$. Activation of enthalpy of (ΔH_{ads}) is calculated from the slope value. The activation of entropy (ΔS_{ads}) is obtained from the equation[11].

$$\boxed{\Delta G_{ads} = \Delta H_{ads} - T\Delta S_{ads}}$$

2.3 Electrochemical measurements

Mild Steel (MS) material was cut into 1 x1 cm^2. The working electrode is molded with Araldite, 1 cm^2 of the working electrode to be immersed into a test solution. The uncovered surface was polished by using various grits of emery paper and using acetone it was degreased. In a test solution, the three electrodes were immersed and steady-state potential was identified and leftover for 20 mines[24]. Using a lugging capillary tube the potential of the electrode which is used (MS) and calomel electrode (SCE) was measured. Throughout the experiments were carried out at room temperature. The resultant current was measured by applying constant potential at an approximate voltage of ± 200 mV. The values of Tafel slopes, βa, βc and current density were obtained by the extrapolation of the values obtained from polarization curves. The inhibition efficiency was calculated using the following formula,

$$\boxed{IE\% = \frac{I_{corr} - I_{corr(i)}}{I_{corr}} \times 100}$$

I_{corr} = Corrosion current density in the absence of inhibitor
$I_{corr(i)}$ = Corrosion current density in the presence of an inhibitor.

A frequency range of 10 kHz to 0.01 Hz was performed for AC impedance study and the same type of electrode set up which is used for potentiodynamic polarization study. R_s- solution resistance and R_t- total resistance were attained between high to low frequency. Which intercepts on the Z' axis, which is associated with the Nyquist plot respectively. Using the formula C_{dl} values were calculated[26].

$$\boxed{IE\% = \frac{R_{ct(i)} - R_{ct}}{R_{ct(i)}} \times 100}$$

2.4 Scanning Electron Microscopy (SEM)

Before testing the SEM, mild steel material was cut into three cubes with a side length of 0.3 cm. Polishing on 400–7000 mesh grit paper which turns the surface into the flat before testing. Two mild steel cubes were separately immersed in 1N HCl in the absence and presence of the inhibitors for 2 hrs at room temperature[26].

3. RESULT AND DISCUSSION

3.1 Synthesis of [4-(4-aminobenzoyl)piperazin-1-yl](furan-2-yl)methanone

The synthesis of [4-(4-aminobenzoyl)piperazin-1-yl](furan-2-yl)methanone is outlined in Scheme 1. 4-nitrobenzoyl chloride was reacted with 1-(2-furoyl) piperazine in the presence of triethylamine to form the [4-(furan-2-carbonyl) piperazin-1yl] (4-nitrophenyl) methanone. The resulting reaction was subjected to a reduction reaction using the reagent $SnCl_2$ to form the compound [4-(4-aminobenzoyl) piperazin-1-yl] (furan-2-yl) methanone.

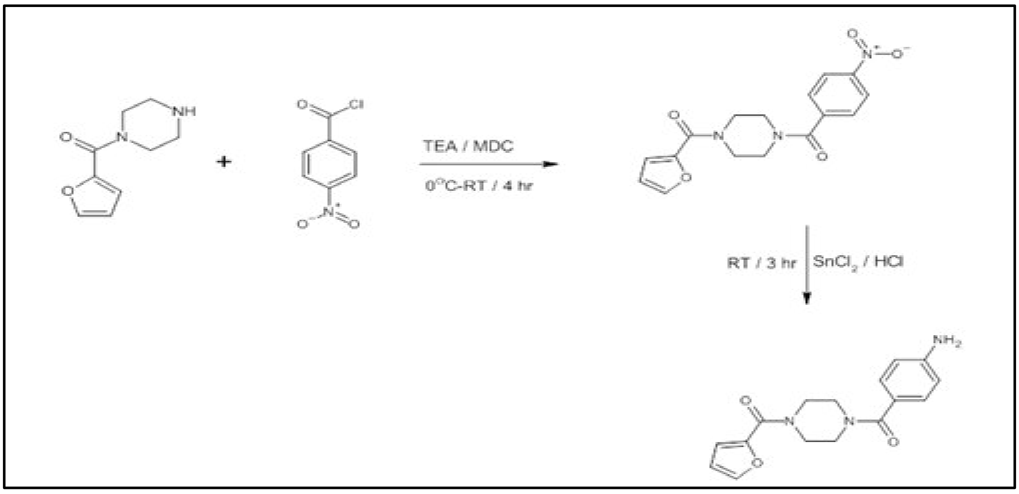

Scheme. 1. Synthesis of [4-(4-aminobenzoyl)piperazin-1-yl](furan-2-yl)methanone

3.1.1 Fourier Transform Infrared Spectroscopy (FT-IR)

The FT-IR spectrum of [4-(furan-2-carbonyl) piperazin-1-yl] (4 nitro phenyl) methanone (Fig. 1) showed absorption bands in 1625 cm^{-1} confirming the presence of carbonyl carbon C=O.

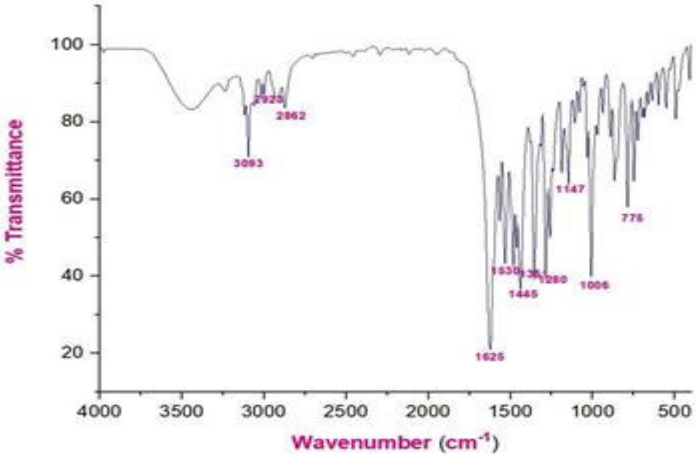

Fig.1. FT-IR spectrum of [4-(furan-2-carbonyl) piperazin-1-yl] (4 nitro phenyl) methanone

The strong band appeared in 1530 cm^{-1} and 1350 cm^{-1}due to NO_2 stretching frequencies. Two bands at stretching frequencies in 2923 cm^{-1} and 2862 cm^{-1} due to CH symmetric and asymmetric frequencies[25], respectively (Fig.1). In the FT-IR spectrum of Fig. 2, reduction of nitro group was confirmed by the disappearance of the NO_2 group absorption band at 1530 cm^{-1} and 1350 cm^{-1} with the appearance of amine NH_2 absorption band[26] at 3334 cm^{-1} and 3221 cm^{-1}. The FT-IR spectrum of Fig. 2 indicated band at 1606 cm^{-1} for C=O stretch[27], 1261 cm^{-1} for C-N stretch[26], and 1171 cm^{-1} for C-O stretching frequencies.

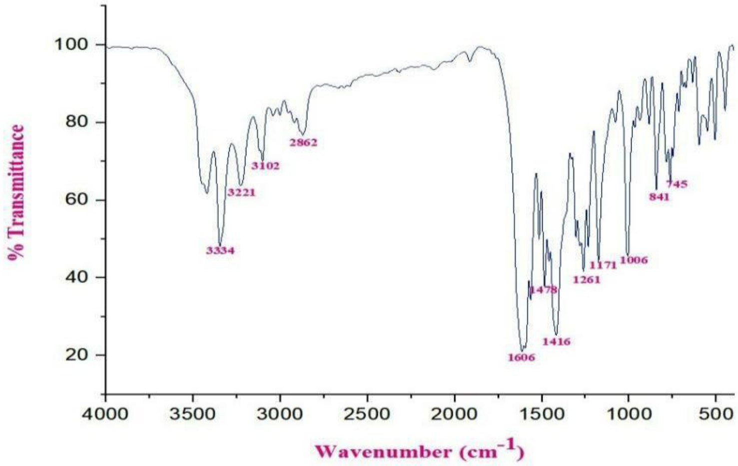

Fig. 2. FT-IR spectrum of [4-(4-aminobenzoyl) piperazin-1-yl] (furan-2-yl) methanone

3.2 *Synthesis of [4-(4-aminophenyl) piperazin-1-yl] (furan-2-yl) methanone*

Synthesis of [4-(4-aminophenyl) piperazin-1-yl] (furan-2-yl) methanone involved a two reaction sequence of nucleophilic aromatic substitution and nitro group reduction. 4-fluoronitrobenzene was first substituted by aromatic nucleophilic displacement with 1-(2-furoyl) piperazine to give the product. The reaction was carried out in the presence of potassium carbonate base and acetonitrile solvent at 70°C. The nitro group of [(furan-2-yl) [4-(4-nitrophenyl) piperazin-1-yl] methanone was reduced by a similar synthetic pattern.

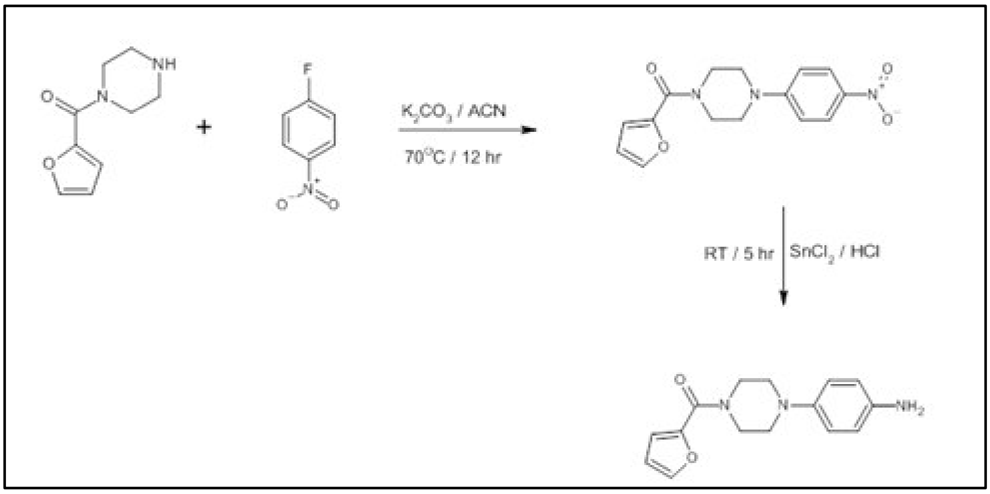

Scheme 2. Synthesis of [4-(4-aminophenyl) piperazin-1-yl] (furan-2-yl)methanone

3.2.1. Fourier Transform Infrared Spectroscopy (FT-IR)

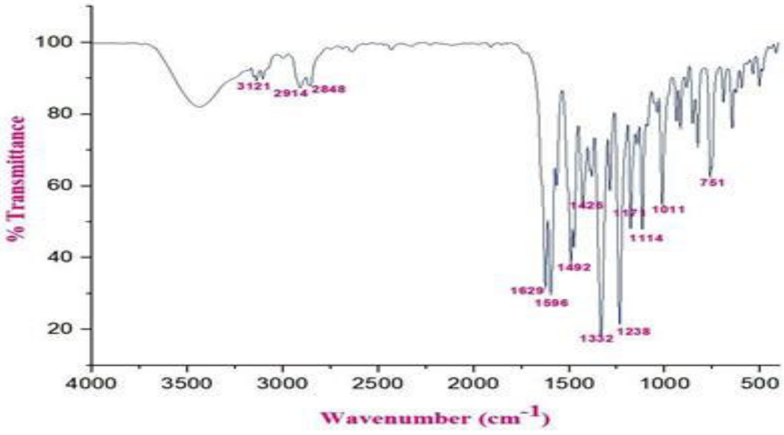

Fig. 3. FT-IR spectrum of [furan-2-yl) 4-(4-nitrophenyl) piperazin-1-yl] methanone

The FT-IR spectrum of [furan-2-yl) 4-(4-nitrophenyl) piperazin-1-yl] methanone showed stretching bands at 1492 cm^{-1} and 1332 cm^{-1} for NO_2 group[28] (Fig.3). The characteristic absorption bands at 1629 cm^{-1} (C=O stretch), 1596cm^{-1} (C-C stretch), 1238cm^{-1} (C-N stretch) and 1171cm^{-1} (C-O stretch) confirmed the expected product. In the FT-IR spectrum of [4-(4-aminophenyl) piperazin-1-yl] (furan-2-yl) methanone, reduction of nitro group was confirmed by the disappearance of the NO_2 group absorption band at 1492 cm^{-1} and 1332 cm^{-1} with the appearance of amine NH_2 absorption band at 3423 cm^{-1}and 3344cm^{-1} (Fig. 4). The FT-IR spectrum of [4-(4-aminophenyl) piperazin-1-yl] (furan-2-yl) methanone indicated band at 1625 cm^{-1} for C=O stretch, 1275 cm^{-1} for C-N stretch, 1176 cm^{-1} for C-O stretch and 940 cm^{-1} bend.

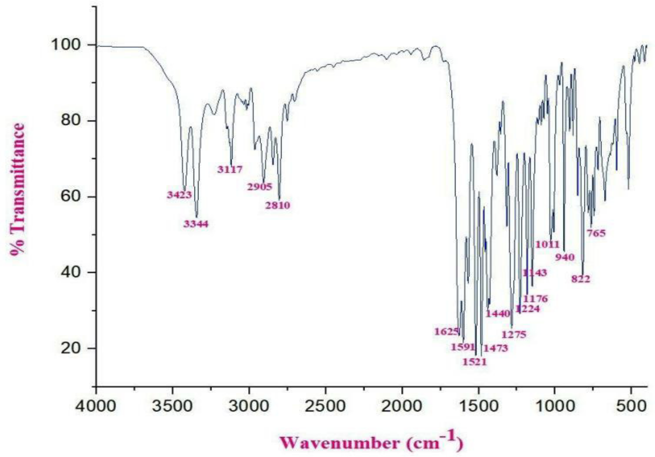

Fig.4. FT-IR spectrum of [4-(4-aminophenyl) piperazin-1-yl] (furan-2-yl) methanone

3.3 *Determination of Corrosion rate, inhibition efficiency (IE), and surface coverage*

The various corrosion parameters such as corrosion rate (CR), inhibition efficiency (IE), and surface coverage were obtained from the weight loss method for mild steel in 1N HCl without and with the various concentrations of (4-4-ABPFM) and (4-4-APFM) inhibitor ranges from 10 ppm to 100 ppm at room temperature for two hours which is tabulated in Table-1. The inhibition efficiency was found to be increased with an increase in the concentration of the inhibitors[29-30].

Table. 1. Weight loss parameters of inhibitors on mild steel corrosion in 1N HCl at room temperature for two hours

Concentration of the inhibitors (ppm)	(4-4-ABPFM)		(4-4-APFM)	
	Rate of corrosion (mmpy)	Inhibition efficiency (%)	Rate of corrosion (mmpy)	Inhibition efficiency (%)
Blank	10.5506	---	23.9989	---
10	7.8988	30.98	19.0028	27.55
20	7.1501	43.66	14.1427	32.50
40	5.8690	49.29	11.4822	39.93
60	4.8295	57.04	11.1032	59.24
80	2.8977	72.53	7.1328	70.27
100	1.2681	80.28	6.4641	73.06

**Inhibition efficiency is 4-4-ABPFM > 4-4-APFM*

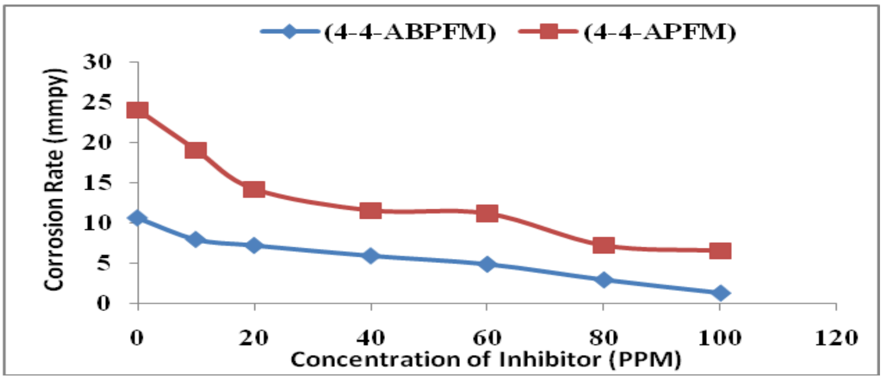

Fig.5. Comparison of Corrosion rate of (4-4-ABPFM) and (4-4-APFM) inhibitor on mild steel at room temperature for two hours

The maximum inhibition efficiency of (4-4-ABPFM) was 80.28 % and for (4-4-APFM) 73.06% was obtained at 100 ppm of an optimum concentration which is due to the formation of a protective layer by the added inhibitors. Fig. 5 and 6 represent the comparison of corrosion rate and inhibition efficiency of (4-4-ABPFM) and (4-4-APFM) inhibitors.

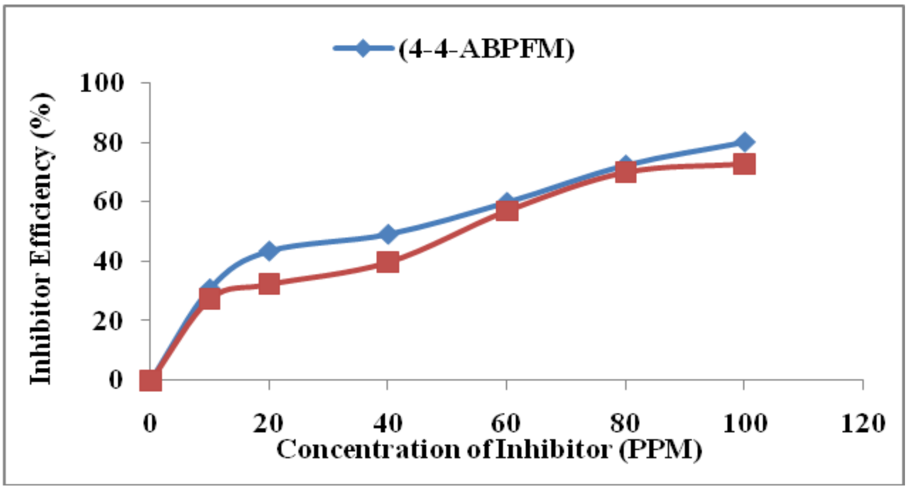

Fig. 6. Comparison of Inhibition Efficiency of (4-4-ABPFM) and (4-4-APFM) inhibitor on mild steel at room temperature for two hours

3.4 *Adsorption isotherm*

Weight loss method were carried out to understand the fundamental information on the interaction between the inhibitors and mild steel surface coverage (θ) which is investigated by the adsorption isotherms with an optimum concentration of (4-4-ABPFM) and (4-4-APFM) in 1N HCl at room temperature for two hours. The values of surface coverage (θ) for optimum concentrations of (4-4-ABPFM) and (4-4-APFM) are given in Table. 2.

Table 2. Langmuir adsorption isotherm for adsorption of (4-4-ABPFM) and (4-4-APFM) on mild steel in 1N HCl

Concentration (M)	Inhibitor	Surface coverage(θ)	ΔG_{ads} KJ / mol^{-1}	K x(10^{-2})
100 PPM	**(4-4-ABPFM)**	0.80	-10.051	1.80
	(4-4-APFM)	0.73	-7.321	1.80

***θ = 4-4-ABPFM (0.80)>4-4-APFM (0.73)**

A plot of C/θ versus C gave a straight line with unit slope suggest that the adsorption of (4-4-ABPFM) and (4-4-APFM) on the metal surface is conforming to Langmuir isotherm[31,32], there is no interactive or repulsive force between the adsorbed molecules and mild steel surface. The adsorption of various concentrations of (4-4-ABPFM) and (4-4-APFM) on the surface of mild steel in 1N HCl solution follows Langmuir adsorption isotherm as shown in Fig. 7.

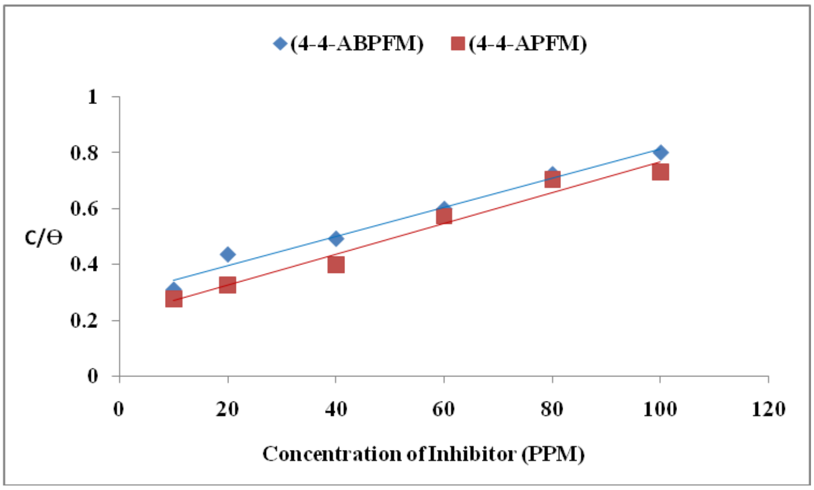

Fig.7. Comparison of Langmuir adsorption isotherm for adsorption of (4-4- ABPFM) and (4-4-APFM) on mild steel in 1N HCl

The adsorption of (4-4-ABPFM) and (4-4-APFM) on a mild steel surface made a blockade for mass and charge transfer. This situation led to the protection of a mild steel surface from the action of aggressive ions in 1N HCl solution. The degree of protection increased with surface coverage by the adsorbed molecules. Therefore the inhibitors show physical and no chemical adsorption. It indicates the force of electrostatic drive of attraction that took place between inhibitor molecules and the surface of the metal. Adsorption of free energy (ΔG_{ads}), in 1N HCl, was found to be -10.051kJmol^{-1} in (4-4-ABPFM) and -7.321 kJmol^{-1} in (4-4-APFM). The values indicate physisorption taken place in these inhibitor systems.

3.5 *Electrochemical measurements*

3.5.1 Potentiodynamic Polarization Studies

Corrosion on mild steel in 1N HCl with the inhibitory effect of 4-4-ABPFM and 4-4-APFM at room temperature was studied using Potentiodynamic polarization studies and it is depicted clearly in Fig. 8 at optimum concentration. Tafel slopes like the Cathodic shift and anodic shift (-βa and -βc) were calculated using polarization values of various potentiodynamic parameters, E_{corr} - corrosion potential and I_{corr} - corrosion current was also calculated. There is a shift in the cathodic region due to the adsorption factor of the inhibitor over the mild steel surface which is observed from the E_{corr}values.

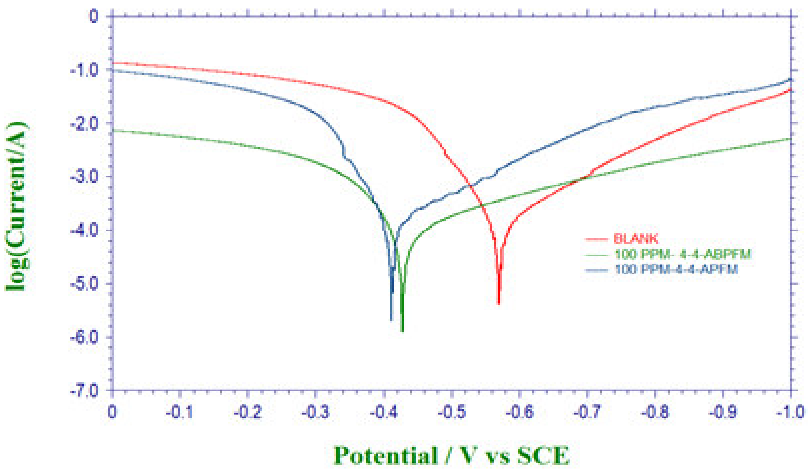

Fig.8. Potentiodynamic polarization curves of mild steel in 1NHCl in the absence and presence of the inhibitors at room temperature

This indicates the controlling nature of the inhibitor which actively blocks the sites on the surface of the metal in an acidic medium. This evidence explains that there is considerable polarization access at the cathode. The inhibitive action of the inhibitor molecule on mild steel in the acidic medium at different temperatures is a cathodic type of inhibitor. From Table. 3 potentiodynamic polarization parameters are represented which shows variability on Tafel slopes and reveals that inhibitor at all concentrations at different temperatures shows the corrosion mechanism process at the cathode[33-35]. At three different temperatures in comparison, I_{corr} values decreased.

Table 3. Polarization parameters of mild steel electrode immersed in the absence and the presence of the inhibitors at room temperature

Name of the Inhibitor	Conc.(ppm)	-βa (mV dec^{-1})	-βc (mV dec^{-1})	Ecorr (mV)	i_{corr} (mA cm^{-2})	Corrosion rate (mmpy)	IE %
	Blank	**7.016**	**5.900**	**-570**	**18.103**	**210.36**	**---**
4-4-ABPFM	100	9.759	4.049	-361	3.432	91.700	81.04
4-4-APFM	100	7.525	4.496	-426	4.213	35.150	76.72

IE % = 4-4-ABPFM (81.04 >4-4-APFM (76.72)

3.5.2 Electrochemical Impedance Studies

The efficiency of the inhibitor EIS - Electrochemical impedance spectroscopy is the best method. This method clearly explains the adhesive nature of the inhibitor over the mild steel surface in a 1N HCl medium. For different corrosion system features of EIS Spectra were shown based on their charge transfer control, diffusion control or a mixer type of inhibitor. From EIS data (Nyquist plot), the mechanism of corrosion can be identified. Electrochemical interface which in term referred to as electrical features can be interpreted using EIS data[36].

Table 4. AC impedance for Mild Steel in 1N HCl medium with 4-4-ABPFM and 4-4-APFM at room temperature.

Name of the Inhibitor	Concentration (ppm)	Rct (Ohm cm^2)	Cdl (μF/ cm^2)	I.E %
	Blank	**22.54**	**805.22**	**---**
4-4-ABPFM	100	81.32	245.65	81.03
4-4-APFM	100	59.84	698.51	62.33

**Rct (Ohm cm^2)4-4-ABPFM (81.32) > 4-4-APFM (59.84)*

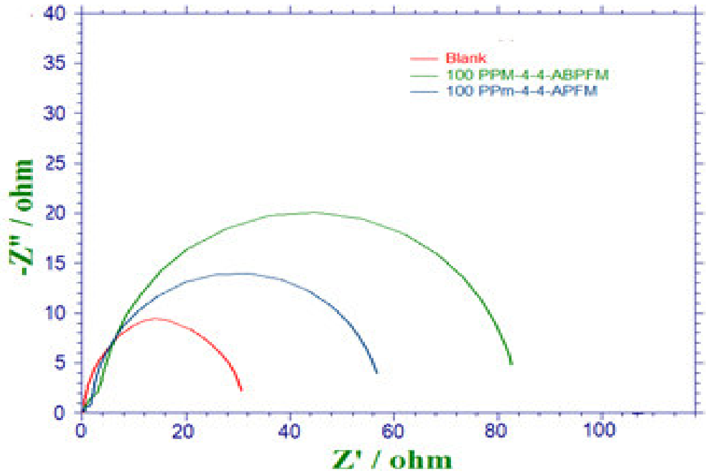

Fig.9. A.C. Impedance curves of mild steel electrode immersed in 1N HCl in the absence and presence of the inhibitors at room temperature

Due to the heterogeneous surface of the surface and roughness of the electrodes are often referred to as dispersion of frequency. The real axis with a semicircle at the center under which gives a Nyquist plot represents the solid electrode's characteristic features37. Nyquist plots for the interface of mild steel electrode and electrolyte with and without inhibitors at optimum concentrations of inhibitors at room temperature were shown in Fig. 9. Impedance parameters were represented in Table. 4. The presence of the N-H group in the inhibitor compound shows better efficiency in the prevention of MS material.

3.6 Scanning Electron Microscopy (SEM)

Surface analysis was carried out by SEM technique to observe the surface conditions of the mild steel in contact with 1N HCl solution.

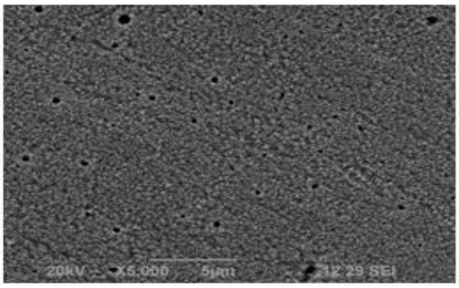

Fig.10. (a) SEM micrograph of mild steel in 1N HCl

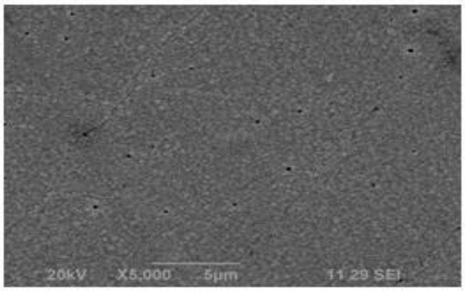

Fig.10. (b) SEM micrograph of mild steel

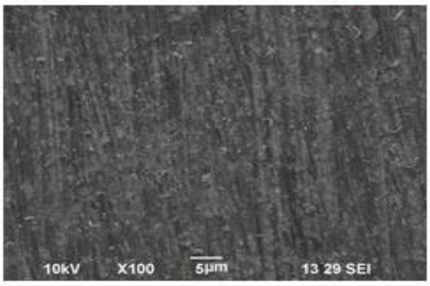

Fig.10.(c) SEM micrograph of in mild 1N HCl with4-4-ABPFM mild steel in 1N HCl with 4-4-APFM

The surface of mild steel specimens without and with 4-4-ABPFM and 4-4-APFM inhibitor concentration was immersed for 2 h at room temperature in the Scanning electron microscope (SEM) with the magnification shown in Fig. 10. (a,b and c). This result is due to the adsorption of inhibitor compounds around the pits. The inert film blocks the active site present on the mild steel surface[38-40].

4 CONCLUSION

The studied organic inhibitors act as excellent corrosion inhibitors for MS in 1N HCl. Investigated for their inhibition performances on mild steel corrosion in 1N HCl solution. The results of both gravimetric and electrochemical experiments showed that all the two compounds inhibit mild steel corrosion in 1N HCl solution and the inhibition efficiency increases with increasing concentration of the inhibitors. The EIS study reveals that the inhibitor functioned via adsorption on metal/solution interface. The potentiodynamic polarization measurements show that (4-4-ABPFM) and (4-4-ABPFM) act as a cathodic inhibitor. The adsorptions of inhibitors were found to follow the Langmuir adsorption isotherm. The results obtained by SEM micrographs. Further, corroborate the formation of protective film on the metal surface. The application of organic inhibitors to inhibit corrosion of mild steel.

5 ACKNOWLEDGEMENTS

The Author expresses their sincere thanks to the Department of Chemistry, Government Arts College (Autonomous), Periyar University, Salem - 636007, Tamilnadu, India for providing the necessary facilities for the successful completion of this research work.

6 AUTHORS CONTRIBUTION STATEMENT

P. Singaravelu and N. Bhadusha conceptualized and gathered the data about this work. V. Dharmalingam these data and necessary inputs were given towards the designing of the manuscript. All authors discussed the methodology, results and contributed to the final manuscript.

7 CONFLICT OF INTEREST

Conflict of interest declared none

8 REFERENCES

1. De la Fuente D, Díaz I, Simancas J, Chico B, Morcillo M. Long-term atmospheric corrosion of mild steel. Corros Sci. 2011;53(2):604-17. doi: 10.1016/j.corsci.2010.10.007.
2. Ulaeto SB, Ekpe UJ, Chidiebere MA, Oguzie EE. Corrosion inhibition of mild steel in hydrochloric acid by acid extracts of Eichhorniacrassipes. Int J Mater Chem. 2012;2:158-64.
3. Sastri VS. Corrosion inhibitors principles and applications. New York: John Wiley and Sons; 1998.
4. Quraishi MA, Singh A, Singh VK, Yadav DK, Singh AK. Green approach to corrosion inhibition of mild steel in hydrochloric acid and sulphuric acid solutions by the extract of Murrayakoenigii leaves. Mater Chem Phys. 2010;122(1):114-22. doi: 10.1016/j.matchemphys.2010.02.066.
5. Caliskan N, Akbas E. Corrosion inhibition of austenitic stainless steel by some pyrimidine compounds in hydrochloric acid. Mater Corros. 2012;63(3):231-7. doi: 10.1002/maco.201005788.
6. Abd El-Maksoud SA, Fouda AS. Some pyridine derivatives as corrosion inhibitors for carbon steel in acidic medium. Mater Chem Phys. 2005;93(1):84-90. doi: 10.1016/j.matchemphys.2005.02.020.
7. Quraishi MA, Sharma HK. 4-amino-3-butyl-5-mercapto-l,2,4-triazole: a new corrosion inhibitor for mild steel in sulphuric acid. Mater Chem Phys. 2002;78:18-21.
8. Ramachandran G, Balamurugan R. Comparative study on mild steel in acidic medium using 5-Amino-2-chloro-3-picoline as inhibitor. Asian J Chem. 2018;30(4):917-9. doi: 10.14233/ajchem.2018.21153.
9. Venkatesan P, Anand B, Matheswaran P. Influence of formazan derivatives on corrosion inhibition of mild steel in hydrochloric acid medium. Chem. 2009;6(s1);Suppl 1:S438-44. doi: 10.1155/2009/507383.
10. Bentiss F, Lebrini M, Lagrenée M. Thermodynamic characterization of metal dissolution and inhibitor adsorption processes in mild steel/2,5-bis(n-thienyl)-1,3,4-thiadiazoles/ hydrochloric acid system. Corros Sci. 2005;47(12):2915-31. doi: 10.1016/j.corsci.2005.05.034.
11. Ansari KR, Quraishi MA, Singh A. Schiff's base of pyridyl substituted triazoles as new and effective corrosion inhibitors for mild steel in hydrochloric acid solution. Corros Sci. 2014;79:5-15. doi: 10.1016/j.corsci.2013.10.009.
12. verma C, Quraishi MA, Olasunkanmi LO, Ebenso EE. l -Proline-promoted synthesis of 2-amino-4-arylquinoline-3-carbonitriles as sustainable corrosion inhibitors for mild steel in 1 M HCl: experimental and computational studies. RSC Adv. 2015;5(104):85417-30. doi: 10.1039/C5RA16982H.
13. Obot IB, Macdonald DD, Gasem ZM. Density functional theory (DFT) as a powerful tool for designing new organic corrosion inhibitors. Part 1: An overview. Corros Sci. 2015;99:1-30. doi: 10.1016/j.corsci.2015.01.037.
14. El Azzouzi M, Aouniti A, Herrag L, Chetouani A, Elmsellem H, Hammouti B. Pharm Chem. 2015;7:12-24.
15. Morad MS, El-Dean AMK. 2,2′-Dithiobis(3-cyano-4,6-dimethylpyridine): A new class of acid corrosion inhibitors for mild steel. Corros Sci. 2006;48(11):3398-412. doi: 10.1016/j.corsci.2005.12.006.
16. Ameer MA, Fekry AM. Inhibition effect of newly synthesized heterocyclic organic molecules on corrosion of steel in alkaline medium containing chloride. Int J Hydrogr Energy. 2010;35(20):11387-96. doi: 10.1016/j.ijhydene.2010.07.071.
17. Abd El-Maksoud SA, Fouda AS. Some pyridine derivatives as corrosion inhibitors for carbon steel in acidic medium. Mater Chem Phys. 2005;93(1):84-90. doi: 10.1016/j.matchemphys.2005.02.020.
18. Thomas JGN. Proceedings of the 5th European symposium on Corrosion Inhibitors. Ann. Universidad Ferrara; 1980. p. 453.
19. Abdallah M. Rhodanineazosulpha drugs as corrosion inhibitors for corrosion of 304 stainless steel in hydrochloric acid solution. Corros Sci. 2002;44(4):717-28. doi: 10.1016/S0010-938X(01)00100-7.

20. Abdallah M. Antibacterial drugs as corrosion inhibitors for corrosion of aluminium in hydrochloric solution. Corros Sci. 2004;46(8):1981-96. doi: 10.1016/j.corsci.2003.09.031.
21. Prabhu RA, Shanbhag AV, Venkatesha TV. Influence of tramadol [2-[(dimethylamino) methyl]-1-(3-methoxyphenyl) cyclohexanol hydrate] on corrosion inhibition of mild steel in acidic media. J ApplElectrochem. 2007;37(4):491-7. doi: 10.1007/s10800-006-9280-2.
22. Okafor PC, Ikpi ME, Uwah IE, Ebenso EE, Ekpe UJ, Umoren SA. Inhibitory action of Phyllanthusamarus extracts on the corrosion of mild steel in acidic media. Corros Sci. 2008;50(8):2310-7. doi: 10.1016/j.corsci.2008.05.009.
23. Noor EA. Potential of aqueous extract of Hibiscus sabdariffa leaves for inhibiting the corrosion of aluminum in alkaline solutions. J ApplElectrochem. 2009;39(9):1465-75. doi: 10.1007/s10800-009-9826-1.
24. Ezhilarasi MR, Prabha B, Santhi T. Novel pyrazole based ionic liquid as a CorrosionInhibitor for mild steel in acidic media. ChemSci Trans. 2015;4(3):1-10.
25. Ananth Kumar S, Sankar A. The chemical synthesis and corrosion inhibitive nature of 2-propyl pentanoic acid doped Poly Ortho Toludine for mild steel in acid medium. Discovery. 2015;36(161):1-10.
26. Dharmalingam V, ArockiaSahayaraj P, John Amalraj A, Pragathiswaran C, Poly. (Acrylic acid) and sodium gluconate as effective corrosion inhibitors for mild steel in chloride environment. Int J ChemTech Res. 2017;10(5):630-41.
27. Singh SK, Zhu C, Vuppuluri V, Son SF, Kaiser RI. Probing the reaction mechanisms involved in the decomposition of solid 1,3,5-trinitro-1,3,5-Triazinane (RDX) by energetic electron. J PhysChem A. 2019;123(44):9479-97. doi: 10.1021/acs.jpca.9b08695, PMID 31589046.
28. Dharmalingam V, ArockiaSahayaraj P, John Amalraj A, AngelinPrema A, Poly. (Acrylic acid) and as effective potassium sodium tartrate inhibitors for mild steel in aqueous environment. J AdvElectrochem. 2016;2(1):37-41.
29. Daoud D, Douadi T, IssaadiSaifi, Chafaa S. Adsorption and corrosion inhibition of new synthesized thiophene Schiff base on mild steel X52 in HCl and H_2SO_4 solutions. Corros Sci. 2014;79:50-8. doi: 10.1016/j.corsci.2013.10.025.
30. Oguzie EE, Li Y, Wang FH. Corrosion inhibition and adsorption behavior of methionine on mild steel in sulfuric acid and synergistic effect of iodide ion. J Coll Interface Sci. 2007;310(1):90-8. doi: 10.1016/j.jcis.2007.01.038, PMID 17331526.
31. Umasankareswari T, Jeyaraj T. Salicylideneaniline as inhibitor for the corrosion of mild steel in 1.0 N hydrochloric acid. J Chem Pharm Res. 2012;4(7):3414-9.
32. Roy P, Karfa P, Adhikari U, Sukul D. Corrosion inhibition of mild steel in acidic medium by polyacrylamide grafted Guar gum with various grafting percentage: effect of intramolecular Synergism. Corros Sci. 2014;88:246-53. doi: 10.1016/j.corsci.2014.07.039.
33. Kuang W, Mathews JA, Macdonald DD. The effect of Anodamine on the corrosion behavior of 1018 mild steelin deionized water: I. Immersion and polarization tests. ElectrochimActa. 2014;127:79-85. doi: 10.1016/j.electacta.2014.02.011.
34. Zheng X, Zhang Shengtao, Gong M, Li W. Experimental and theoretical study on the corrosion inhibition of mild steel by 1-Octyl-3-methylimidazolium L-Prolinate in sulfuric acid solution. IndEngChem Res. 2014;53(42):16349-58. doi: 10.1021/ie502578q.
35. de Souza FS, Spinelli A. Caffeic acid as a green corrosion inhibitor for mild steel. Corros Sci. 2009;51(3):642-9. doi: 10.1016/j.corsci.2008.12.013.
36. Badiea AM, Mohana KN. Corrosion mechanism of low-carbon steel in industrial water and adsorption thermodynamics in the presence of some plant extracts. J Mater Eng Perform. 2009;18(9):1264-71. doi: 10.1007/s11665-009-9378-x.
37. Dharmalingam V, ArockiaSahayaraj P, John Amalraj A, Rajendran S. Electrochemical study and spectroscopic methods used for self assemblingnanofilm formed by polyacrylic acid on mild steel in aqueous environment. Asian J Res Chem. 2016;9(1):40-6.
38. Singh P, Srivastava V, Quraishi MA. Novel quinoline derivatives as green corrosion inhibitors for mild steel in acidic medium: electrochemical, SEM, AFM, and XPS studies. J Mol Liq. 2016;216:164-73. doi: 10.1016/j.molliq.2015.12.086.
39. XieFangxia, He X, Lv Y, Wu M, He X, Qu X. Selective laser sintered porous Ti–(4-10) Mo alloys for biomedical applications: structural characteristics, mechanical properties and corrosion behaviour. Corros Sci. 2015;95:117-24. doi: 10.1016/j.corsci.2015.03.005.